

Finite Element Simulation of a Scoliotic Spine with Periodic Adjustments of an Attached Growing Rod

O. A. Abolaeha, J. Weber, and L. T. Ross

Abstract- Early Onset Scoliosis (EOS) is a deformity of spine which occurs during growth. Spinal growing rod instrumentation is currently a procedure of early onset scoliosis management and newer technologies to treat scoliosis without fusion hold the exciting promise of a new paradigm in spinal deformity care. A Finite Element Model (FEM) of a scoliotic spine was created and enhanced to simulate spine growth after the attachment of a growing rod. Growing rod instrumentation was included utilizing FEA to accurately simulate the required 3D forces and moments to achieve the desired correction. We measured forces on the rods and the spine during adjustment periods (for correction of the spinal deformity) and during growth periods. For this study, a two-year period was simulated with adjustments at six month intervals. The FEM allowed us to collect data during growth periods from sensors which are only accessible during the surgical procedures.

I. INTRODUCTION

Early Onset Scoliosis (EOS) is a deformity of the growing spine, affecting children before the age of complete lung growth. The deformities are well described in humans and associate a coronal curvature, a hypokyphosis in the sagittal plane and a vertebral rotation in the axial plane. If left untreated, the progressive and severe spinal deformity associated with the EOS can have significant health consequences such as pain, medical complications, physical discomfort, and breathing problems that require some form of treatment [1].

One current treatment for EOS involves implanting growing rod instruments, using either single or dual rods. This has proven to be effective in controlling the deformities and allowing for spinal and lung growth [2-5]. In a typical growing rod implant surgery, the rods are attached along both sides of the spine above and below the curve using pedicle screws and hooks Fig. 1. The rod is then extended to correct the curvature until the surgeon feels enough compression in the rod to stop the adjustment. The curve can usually be corrected by fifty percent at the time of the initial surgery. After the first operation, the patient must undergo invasive

lengthening procedures (known as distractions) every six months to a year in order keep up with the spine growth. These distractions must be repeated over a typical implantation period of five to ten years [1].

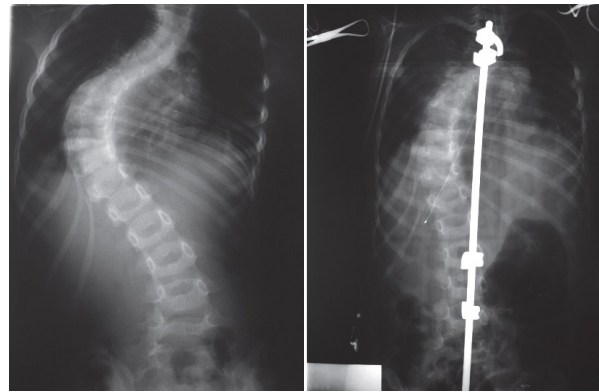


Figure 1. Pre-surgical (left) and post-surgical (right) radiographs.

A finite element analysis (FEA) of the spine deformity correction has made an important contribution to our understanding of the biomechanical behavior of the human scoliotic spine and its mechanisms [6]. Subbaraj et al created a presurgical spine Finite Element Model (FEM) to simulate the Luque system (Luque rods), which demonstrates comparable results to post-surgical scoliosis correction procedure [7]. Based on the Hueter-Volkman law for bone growth modulation, recent research approaches have utilized FEA in order to simulate the progression of non-instrumented idiopathic scoliosis [8-10]. Mark et al. has modeled the growth modulation corrective techniques in pediatric scoliosis using the finite element method [11]. However, to our knowledge, the finite element method has not been applied to simulate the spine growing rod behavior in the typical surgical procedure.

The objective of the present study was to explore and simulate the method of single *growing rod* instrumentation in human scoliotic FEM by quantifying the required force that must be applied to achieve the desired correction (desired Cobb angle) of the EOS. Furthermore, more data regarding the change of corrective force and the spine growth over a period of time will be captured and recorded from the model. This data will provide significant insight in support of the development of a motorized elongation device.

*Research supported by the Graduate school at University of Dayton

O. A. Abolaeha PhD is student with the Electrical Engineering Department, University of Dayton, Dayton, OH 45469 USA, (e-mail: abolacha@gmail.com).

J. G. Weber, PhD, Associate Dean with School of Engineering, University of Dayton, Dayton, OH 45469 USA, (e-mail: john.weber@notes.udayton.edu).

L. T. Ross, Ph.D., P.E. Electronics Engineer AMB Surgical, address: 3634 Noble Way Franklin Ohio 45005, (e-mail: tross007@cinci.rr.com).

II. MATERIAL AND METHODS

A. Finite element model

The geometry of spine finite element model was constructed from published studies by Bertand et al [12]. The model is composed of 17 vertebral bodies (T1-L5) and 16 intervertebral discs using linear, homogeneous and isotropic material properties, their values are presented in (Table I) [9, 11]. The SFEM was developed utilizing Abaqus 6.11-1 (Dassault Systemes). The scoliotic model exhibits a right thoracic curve Cobb angle of 37° with normal sagittal profiles. Internal components of the SFEM consider physiological structures of the spinal column. Every vertebra was created as a wedged cylinder that consists of cortical and cancellous bone and three sections of vertebral growth plates, namely: the sensitive zone, the newly formed bone zone, and the transition zone [9] Fig. 2. The intervertebral disc contains the annulus fibrosis, and nucleus pulposus. Internal components divisions of the models have been taken from published studies: 0.64 mm thick cortical shell, 0.62 mm growth plate (immature endplate), a nucleus cross-sectional area proportion of 45% [11]. The anterior-posterior longitudinal ligaments were modeled with truss elements to be active in tension under stress (1, 1.76 MPa) respectively [13]. This model contains 94,818 nodes and 68,479 elements representing vertebral and intervertebral discs by linear hexahedral elements of type C3D8I and hooks and screw by quadratic tetrahedral elements of type C3D10I. To simulate body loading, a distributed load is applied to each vertebral body as previously published by Schultz [14], beginning with a body weight (BW) distribution of 14% on T1 with an addition of 2.6% on each successive vertebral body, ending at L5, which will bear of 57% of BW.

	Zone	Young's modulus (MPa)	Poisson's ratio
Vertebral body	Cortical bone	14,500	0.3
	Cancellous bone	400	0.3
Growth plate	Sensitive zone	12	0.4
	Newly formed bone	100	0.3
	Transition zone	300	0.3
Intervertebral disc	Nucleus	2	0.49
	Annulus	8	0.45
Ligaments	Anterior longitudinal ligament (Area= 38 mm ²)	20	0.3
	Posterior longitudinal ligament (Area = 20 mm ²)	70	0.3
Growing Rod	Stainless steel	190,000	0.4

Table I. Mechanical properties of the finite element model

The inferior extremity of L5 was restrained in all degrees of freedom during loading and spine growth simulation steps. The superior extremity of T1 was free to displace vertically along the axis of growth, but was constrained in the off-axes.

B. Model of spinal growth

Abnormal spinal growth was described in detail by Stokes [15], which is briefly summarized in this paper. In this approach, the stresses present in the sensitive zone of the vertebral growth plate determine the local bone growth (bone calcification) in the newly formed bone layer. The transition layer connects the sensitive and the newly formed bone layers to the completely formed bone. The amount of the actual growth G was computed as the product of normal growth G_m and a regularization, which was represented by the scaled difference between the stress on the growth plate (σ) of the scoliotic spine and that under regular conditions (σ_m) of the normal spine: $G = G_m(1 - \beta(\sigma - \sigma_m))$ (1) where β = parameter giving the sensitive of bone growth modulation to the applied stress. Once the stress in the sensitive zone was calculated, the local growth of the elements of the newly formed bone layer within the growth plate was simulated using the thermal expansion.

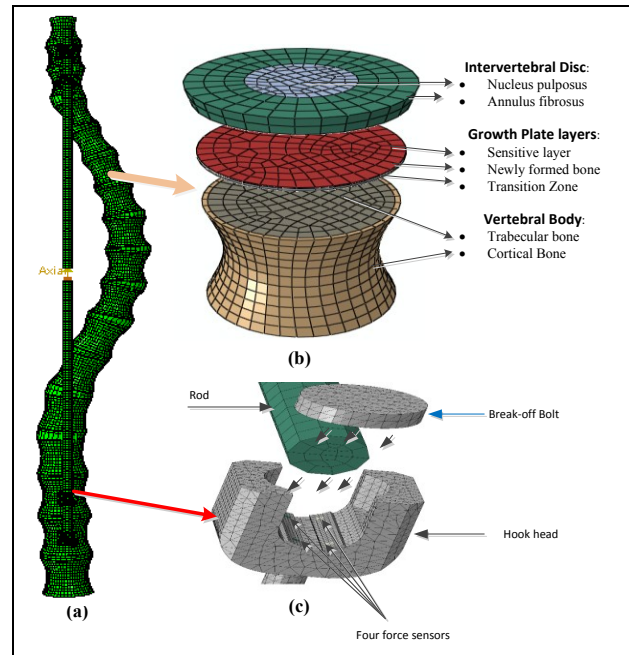


Figure 2. (a) Posterior-anterior views of the instrumented scoliotic finite element model. (b) The modeling of intervertebral disc, growth plate zones, and the vertebral body in the spinal column model were modeled similar to Lin Shi et al [10]. (c) FEM for growing rod instrumentation.

The amount of growth must be calculated for each individual vertebra in order to get the global result of the spine growth. For this work, the following growth parameters were used.

$$G_m = 0.8 - 1.1 \text{ mm year}^{-1}$$

$$\beta = 1.3 \text{ MPa}^{-1}$$

$$\sigma_m = 0.5 \text{ MPa.}$$

These parameters were adopted from previous simulation models that were created and validated using current patient data for the purpose of using the FEA to simulate the growth of the non-instrumented scoliotic model [10, 16].

C. Model of growing Rod instrumentation

Instruments to quantify 3D forces and moments applied by orthopedic surgeons have been reported [17, 18]. The sensor instrument was created to retrofit the hook instrumentation in order to increase surgical outcome and patient safety. In order to simulate the global forces and moments applied by the surgeon during and after surgery procedure, the FEA model was updated by incorporating more complex growing rod instruments to determine the force and moments in 3D relative to Benfield et al [17] sensor method Fig. 2(c). In brief, the FEA model concepts are shown in Fig. 3 where the forces on each hook are measured by two sensors strips, lying parallel to the rod, spanning along width of notch hook, and contacting the rod at 30° angles. Due to the complex loading on the rod, reaction loads distributed onto the strips include shear and normal force distributions that vary on the entire length of the strip. In this study, measuring the forces and moments at the interfaces between the rod and hook or screw (on specify element sets) are given by python script code according to the follow equations using coordinate systems shown in Fig. 3.

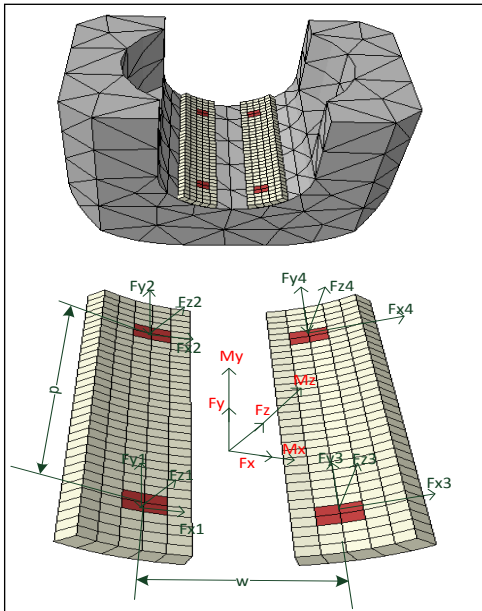


Figure 3. The FEA model of hooks and screws shows coordinate systems to capture forces and moments component as proposed by Benfield et al [17].

$$F_x = \sum_{n=1}^4 F_{x_n} \quad (2)$$

$$F_y = \sum_{n=1}^4 F_{y_n} \quad (3)$$

$$F_z = \sum_{n=1}^4 F_{z_n} \quad (4)$$

$$M_x = \frac{d}{2} (F_{z_1} + F_{z_3} - F_{z_2} - F_{z_4}) \quad (5)$$

$$M_y = \frac{w}{2} (F_{z_3} + F_{z_4} - F_{z_2} - F_{z_1}) \quad (6)$$

$$M_z = \frac{d}{2} (F_{x_1} + F_{x_4} - F_{x_3} - F_{x_2}) + \frac{w}{2} (F_{y_1} + F_{y_2} - F_{y_3} - F_{y_4}) \quad (7)$$

The stainless steel materials properties were assigned to growing rod instrumentation model, representing the basic material types used for interbody implants (Table I).

The scoliotic spine model was modified by fusion of the growing rod on the (T2-T3) vertebral pair and the (L3-L4) pair. The rod is attached to both vertebrae in the pair to distribute the load, which is identical to current surgical insertion procedure. The growing rod was modeled to expand and maintain the compressive force on the rod that results from simulation of the surgical correction procedure. After the single growing rod was inserted into the scoliotic FE model, the next goal was to simulate the longitudinal extension of the rod beginning with the initial surgery. Once the rod is placed and extended, the growth over a 2-year period was simulated. Similar to the actual medical protocol, the lengthening operation was modeled to make adjustments to the rod on a semiannual basis. This period was simulated using the steps as shown in the flowchart diagram Fig. 4.

III. RESULTS

From Fig. 4, step 2 represents the implantation of the rod and the initial adjustment to achieve the desired Cobb angle. The length of the rod was adjusted until the Cobb angle was reduced from an initial value of 37° to 28°. This required the rod to be lengthened by 5 mm, resulting in a corrective force of 362 N. Table 2 shows the force required to lengthen the rod and the effect on the Cobb angle at of our procedure steps.

Steps # 2,4,5,6,7	Rod distractor (mm)	Distraction force (N)	Cobb angle (θ°)	
			before	after
<i>Initial Adjustment</i>	5	362	37	28
<i>After 1st growth period</i>	10	669	42	34
<i>After 2nd growth period</i>	17	942	40	33
<i>After 3rd growth period</i>	20	1215	39	37
<i>After 4th growth period</i>	30	1454	49	40

Table II. Distraction Force and Cobb Angle for the Correction Procedure

Step 3 modeled the growth of the spine over a six month period. During this simulated growth period, we measured growth of the spine, the Cobb angle and the force on the growing rod. The spine grew approximately 12 mm during this period and the Cobb angle changed by approximately 14°. The force on the growing rod was reduced to approximately 669 N.

Steps 2 and 4 through 6 repeated the cycle of adjustment of the rod and growing the spine to cover a two-year period. Step seven adjusted the spine after the final simulated growth period. Fig. 5 shows the progression of the growth and the resultant Cobb angles and rod lengths.

The global forces and moments acting on one of the growing rod hooks are shown in Fig. 6. This chart was derived by modeling the sensors used by Benfield et al [17] and incorporating them in the FEM. The FEM allowed us to view the magnitude of force and moments applied by surgeon to vertebra during the spine correction procedure and spine growth periods. However, since the sensor is still under development, sensor data is not available to us to compare with our FEM result as yet.

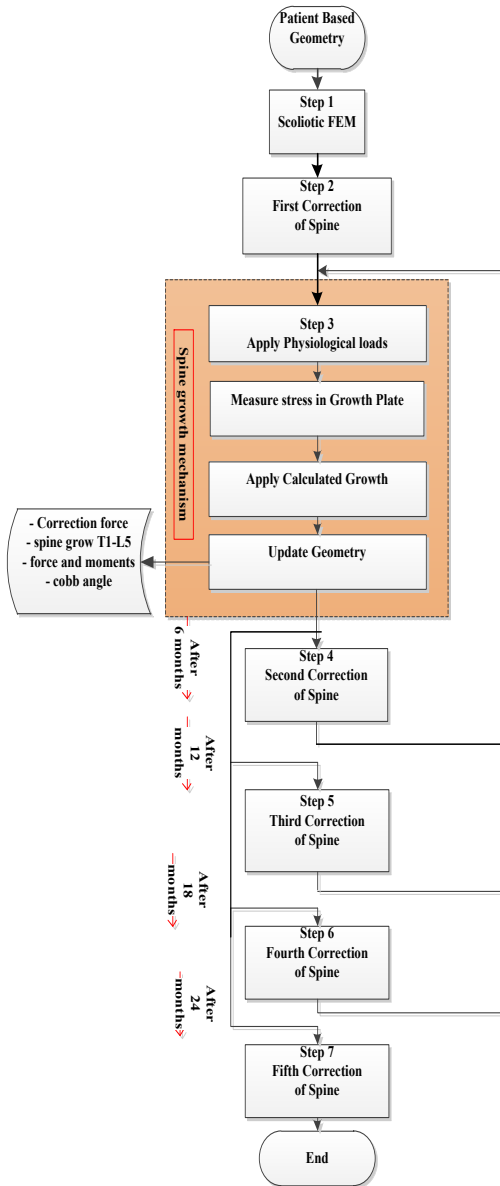


Figure 4. Flowchart diagram shows the simulation sequence steps pattern of single growing rod correction procedure.

IV. Discussion and Conclusions

The complete process for a two-year spine growth period was modeled with results presented in Figure 5. The forces to effect the required Cobb angle changes appear to correlate well with patient data reported by Teli et al and Noordeen et

al [19, 20]. For instance, Teli [19] reported that the measured magnitude of force generated during the 5mm distraction process ranged from 172 N to 447 N. The force found in the FEM for the same 5 mm growing rod distraction is 362 N, which lies within this range. However, FEM force measured 669 N with growing rod distraction of 10 mm, which is slightly higher than Teli's [19] value of 500 N for the same amount of rod displacement. From Table (II), we can see clearly that distraction force is increasing significantly each time growing rod distraction is attempted. This increase is similar to Noordeen's et al [20] conclusion regarding increasing distraction forces (measured over 60 consecutive lengthening procedures in 26 patients). In addition, the growth exhibited by our model of the scoliotic spine mirrors that reported by Akbarnia, et al [1] from patient data. This is an important consideration for the development of growing rod structures. By having a high fidelity model of the spine, we are able to explore enhanced growing rod configurations very rapidly and eliminate those that would not perform well. The model of the spine allowed us to gather data on the forces acting on the spine during both the simulated surgical procedures and during the growth period. These force values are key to the development of growing rod systems which can be adjusted without invasive surgical procedures. Sensing the forces on the spine and understanding the relationship between the force and the Cobb angle will allow us to move forward with enhanced systems.

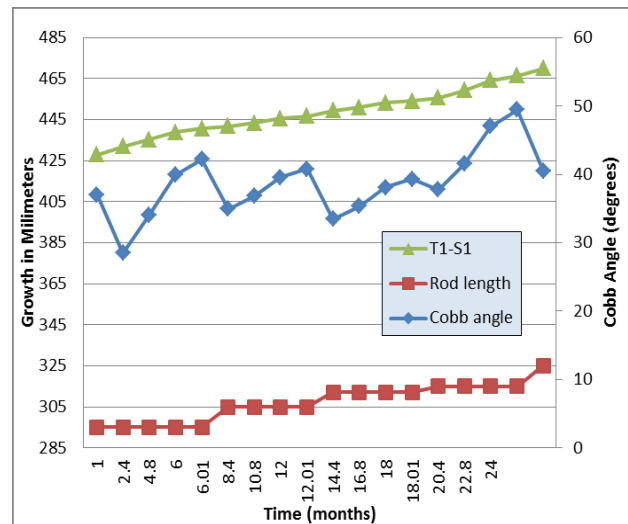


Figure 5. Results from FEM for simulated two-year growth.

Future work: The results presented here are from the upgraded preliminary finite element model. The next generation model will include nonlinear geometric effects. Further efforts are required to fully validate this model. However, the preliminary results are very promising.

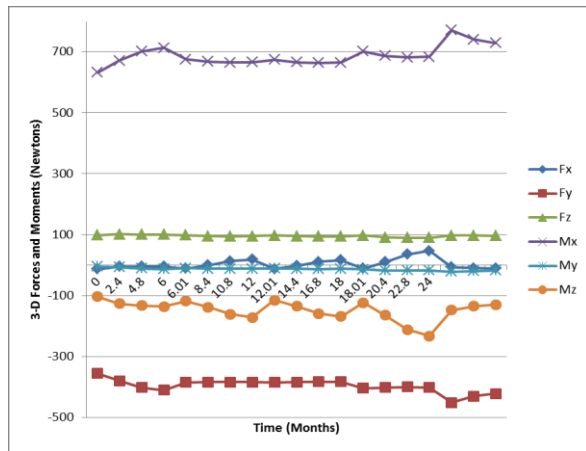


Figure 6. 3-D forces and moments on one of the growing rod hooks.

REFERENCES

[1] B. A. Akbarnia, M. Yazici and G. H. Thompson, *The Growing Spine*. Heidelberg: Springer, 2011.

[2] G. H. Thompson, B. A. Akbarnia, P. Kostial, C. Poe-Kochert, D. G. Armstrong, J. Roh, R. Lowe, M. A. Asher and D. S. Marks, "Comparison of single and dual growing rod techniques followed through definitive surgery: a preliminary study," *Spine (Phila Pa 1976)*, vol. 30, pp. 2039-2044, 09/15, 2005.

[3] G. H. Thompson, B. A. Akbarnia and Campbell, Robert M., Jr, "Growing rod techniques in early-onset scoliosis," *J. Pediatr. Orthop.*, vol. 27, pp. 354-361, 2007, 2007.

[4] A. Torre-Healy and A. F. Samdani, "Newer technologies for the treatment of scoliosis in the growing spine," *Neurosurg. Clin. N. Am.*, vol. 18, pp. 697-705, 10, 2007.

[5] H. B. Elsebai, M. Yazici, G. H. Thompson, J. B. Emans, D. L. Skaggs, A. H. Crawford, L. I. Karlin, R. E. McCarthy, C. Poe-Kochert, P. Kostial and B. A. Akbarnia, "Safety and efficacy of growing rod technique for pediatric congenital spinal deformities," *J. Pediatr. Orthop.*, vol. 31, pp. 1-5, 2011, 2011.

[6] A. C. Jones and R. K. Wilcox, "Finite element analysis of the spine: towards a framework of verification, validation and sensitivity analysis," *Med. Eng. Phys.*, vol. 30, pp. 1287-1304, 12, 2008.

[7] K. Subbaraj, D. N. Ghista and G. R. Viviani, "Presurgical finite element simulation of scoliosis correction," *J. Biomed. Eng.*, vol. 11, pp. 9-18, 01, 1989.

[8] I. Villemure, C. E. Aubin, J. Dansereau and H. Labelle, "Simulation of progressive deformities in adolescent idiopathic scoliosis using a biomechanical model integrating vertebral growth modulation," *J. Biomech. Eng.*, vol. 124, pp. 784-790, 12, 2002.

[9] P. Sylvestre, I. Villemure and C. Aubin, "Finite element modeling of the growth plate in a detailed spine model," *Medical and Biological Engineering and Computing*, vol. 45, pp. 977-988, 2007.

[10] L. Shi, D. Wang, M. Driscoll, I. Villemure, W. C. Chu, J. C. Cheng and C. Aubin, "Biomechanical analysis and modeling of different vertebral growth patterns in adolescent idiopathic scoliosis and healthy subjects," *Scoliosis*, vol. 6, pp. 11-11, 05/23, 2011.

[11] M. Driscoll, C. Aubin, A. Moreau and S. Parent, "Biomechanical comparison of fusionless growth modulation corrective techniques in pediatric scoliosis," *Medical and Biological Engineering and Computing*, vol. 49, pp. 1437-1445, 2011.

[12] S. Bertrand, W. Skalli, L. Delacherie, D. Bonneau, G. Kalifa and D. Mitton, "External and internal geometry of European adults," *Ergonomics*, vol. 49, pp. 1547-1564, 12/15, 2006.

[13] J. Chazal, A. Tanguy, M. Bourges, G. Gaurel, G. Escande, M. Guillot and G. Vanneuville, "Biomechanical properties of spinal ligaments and a histological study of the supraspinal ligament in traction," *J. Biomech.*, vol. 18, pp. 167-176, 1985.

[14] A. B. Schultz, G. B. J. Andersson, K. Haderspeck, R. Örtengren, M. Nordin and R. Björk, "Analysis and measurement of lumbar trunk

loads in tasks involving bends and twists," *J. Biomech.*, vol. 15, pp. 669-675, 1982.

[15] I. A. Stokes, H. Spence, D. D. Aronsson and N. Kilmer, "Mechanical modulation of vertebral body growth. Implications for scoliosis progression," *Spine (Phila Pa 1976)*, vol. 21, pp. 1162-1167, 05/15, 1996.

[16] M. Driscoll, C. Aubin, A. Moreau, I. Villemure and S. Parent, "The role of spinal concave-convex biases in the progression of idiopathic scoliosis," *Eur. Spine J.*, vol. 18, pp. 180-187, 02, 2009.

[17] D. Benfield, E. Lou and W. Moussa, "Development of a MEMS-based sensor array to characterise in situ loads during scoliosis correction surgery," *Comput. Methods Biomech. Biomed. Engin.*, vol. 11, pp. 335-350, 08, 2008.

[18] E. Lou, V. J. Raso, B. Martin, D. Shile, M. Epper, J. K. Mahood, M. Moreau and D. L. Hill, "Wireless surgical tools for mechanical measurements during scoliosis surgery," in *Engineering in Medicine and Biology Society, 2005. IEEE-EMBS 2005. 27th Annual International Conference of the*, 2005, pp. 7131-7134.

[19] M. Teli, G. Grava, V. Solomon, G. Androletti, E. Grismondi and J. Meswania, "Measurement of forces generated during distraction of growing-rods in early onset scoliosis," *World J Orthop*, vol. 3, pp. 15-19, 02/18, 2012.

[20] H. M. Noordeen, S. A. Shah, H. B. Elsebaie, E. Garrido, N. Farooq and M. Al Mukhtar, "In vivo distraction force and length measurements of growing rods: which factors influence the ability to lengthen?" *Spine (Phila Pa 1976)*, vol. 36, pp. 2299-2303, 12/15, 2011.